Hindawi
Advances in Condensed Matter Physics
Volume 2023, Article ID 9518475, 13 pages
https://doi.org/10.1155/2023/9518475

Research Article

Variation of Bulk Modulus, Its First Pressure Derivative, and Thermal Expansion Coefficient with Applied High Hydrostatic Pressure

Manaf A. Mahammed [1] **and Hamsa B. Mohammed** [2]

[1] *Department of Physics, College of Science, University of Duhok, Duhok, Iraq*
[2] *Environmental Techniques Department, Environmental Science College, University of Mosul, Mosul, Iraq*

Correspondence should be addressed to Manaf A. Mahammed; manaf.zivingy@uod.ac

Received 26 December 2022; Revised 27 July 2023; Accepted 31 August 2023; Published 12 October 2023

Academic Editor: Sergio Ulloa

Throughout this work, the equations of variation of the isothermal bulk modulus, its first pressure derivative, and the volumetric thermal expansion coefficient as a function of pressure were derived based on the Birch–Murnaghan equation of state (B–M EOS). The bulk modulus and its first derivative at ambient temperature for nine elements were extracted by fitting the published experimental pressure–volume data to B–M EOS, and the results were compared with other published researches, and there was a good agreement. Moreover, those extracted values were used to study the variation of the isothermal bulk modulus, its first pressure derivative, and the isothermal coefficient of thermal expansion as a function of the applied hydrostatic pressure using the equations that were derived from this work.

1. Introduction

Researches concerning materials under high pressure helps to understand the thermoelastic properties of solid materials and find widespread applications in high-pressure physics, material sciences, geoscience, planetary, and astrophysics since the application of high pressure is a very efficient tool to make a unique modification in structure, behavior, as well as properties of the material. In addition, it helps to understand the nature of solids that have been subjected to high pressure and temperature [1, 2], relatively high hydrostatic pressure. The compression of solids under relatively high hydrostatic pressure can make significant effects on some of their properties [3–5]. Those properties include the interatomic lattice structure and thermal, electronic, mechanical, and optical properties. Velisavljevic et al. [6] studied the structural and electrical properties of Be under hydrostatic pressure up to 66 GPa using X-ray diffraction (XRD), and there was no evidence of transition from hcp up to volume compression $V/V_0 = 0.708$. They fitted their data to adapted polynomial second order equation of state (AP2-EOS), and they got values of bulk modulus $B_0 = 106.5$ GPa and pressure derivative of bulk modulus $B_0' = 3.541$ [6]. Evans et al. [7] measured the Raman phonon and lattice constants of Be up to 80 and 180 GPa hydrostatic pressure, respectively, and they determined the values $B_0 = 109.88$ GPa and $B_0' = 3.584$, respectively. Also, they noticed the increasing of c/a ratio with pressure reaching 1.6 when the pressure increased to 180 GPa. Nakano et al. [8] performed XRD experiments on Be element under high pressure to 171 GPa, and they determined the EOS of hcp–Be by fitting their diffraction data to Birch–Murnaghan (B–M EOS) and extracted the values $B_0 = 97.2 \pm 2.5$ GPa and $B_0' = 3.61 \pm 0.07$. Their data also revealed the stability of hcp phase of Be under compression up to 171 GPa. Potassium K belongs to alkali metals at ambient condition, crystalizes in bcc structure, and converts to fcc structure at 11.6 GPa [9, 10]. The phase transition sequence of K has been studied by Lundegaard et al. [11] and Degtyareva [10], using a combination of X-ray powder and single crystal diffraction. Fujihisa and Takemura [12] performed diffraction experiments on the hcp–Co under pressure to 79 GPa by using diamond anvil cell (DAC) and imaging plate. The determined value of

$B_0 = 199 \pm 6$ GPa and that of $B_0' = 3.6 \pm 0.2$. The use of fcc phase of Al in the dual role of pressure standard and solid pressure-transmitting medium (PTM) up to 200 GPa has been discussed by Singh [13] by using XRD patterns with (DAC), and the results showed that Al has all the properties required for a PTM and pressure standard. Molybdenum (Mo) is a bcc 4d transition metal with wide engineering and technology applications for its thermal and mechanical strength. It is also widely used as a pressure standard in DAC [14–16]. The P–V–T EOS of bcc-Mo have been investigated at pressure 31 GPa using XRD measurements by Litasov et al. [16], and data analysis was performed using B–M EOS and MGD approaches combined with Vinet EOS and obtained similar results for both of two equations at pressure below 1 Mbar while significant deviation may occur at higher pressure. Ko et al. [17] used XRD to measure the EOS and mechanical properties of copper (Cu) under high pressure. Their measured value for the bulk modulus of pure crystalline Cu was 15% less than the previously published values. They attributed the large values of the bulk modulus of the Cu that were published previously to the existence of defects or imperfections such as vacancy, interstitial, substitutional defects, and dislocations that make the materials harder than materials without it [17]. Tantalum (Ta) is a bcc with high ductility and thermal, mechanical, and chemical stability, so it is important for using in jet engines and electronic devices and could be a good candidate for an internal pressure standard for static high-pressure researchers [18]. Cynn and Yoo [18] investigated the volume compression of Ta metal by using angle-resolved synchrotron XRD with (DAC) and confirmed that the bcc phase of Ta is stable to 174 GPa. Gold (Au) is usually used as an internal pressure calibrant because of its stable fcc structure at extremely high pressure and temperature [19, 20]. Güler and Güler [5] used embedded atom method (EAM)-based geometry optimization calculation to study effects of pressure on elastic constants, bulk modulus, shear modulus, and young modulus of Au at 1,000 GPa, and the results showed that all the elastic constants increased almost linearly with increasing pressure. Tungsten (W) is a 5d transition metal that is characterized by its highest melting point, and it crystallizes in bcc structure and it is also stable up to extremely high pressure at room temperature. Jiang et al. [21] studied the structural, mechanical, electronic, and thermodynamic properties of W under different pressures by using the first-principles method and showed that W metal is stable up to 100 GPa.

At absolute 0 k as well as at finite temperature and due to thermal fluctuations, the crystalline solids atoms make small vibrations about their equilibrium positions. The crystal binding energy can be expressed as an expansion of power series in terms of the displacements of those atoms from their equilibrium positions. When the terms beyond the quadratic ones are neglected, then this will be referred to as harmonic approximation, and the vibration is known as harmonic lattice vibration [22]. Among the consequences of harmonic approximation, no thermal expansion can take place, the elastic constants will no longer depend upon pressure and temperature as well as the heat capacity tends to be constant at high temperatures [23]. While for real crystals, none of the abovementioned consequences is satisfied exactly. This happens when terms of lattice binding energy higher than the quadratic ones are taken into consideration, and this is referred to as anharmonic approximation and the lattice vibration is known as anharmonic lattice vibration [24, 25]. Kazanc and Ozgen [26] investigated the changes of acoustic phonon frequencies with hydrostatic pressure for Cu, Ni, Al, Ag, and Au transition metals using molecular dynamics MD simulations based on EAM. Their results show that the pressure causes an increment in phonon frequency and that this increment does not vary linearly with the increased pressure. Jalal et al. [27] used Suzuki and B–M EOSs to study the effect of hydrostatic pressure on two Si nanoparticles. They showed that the volume compression ratio of the smaller nanoparticle was greater, and the shift in its phonon frequency spectrum was more significant. They attributed that to the higher bulk modulus of the smaller silicon nanoparticle [27]. AL-Faris et al. [28] made theoretical calculations to study the thermodynamic properties of gallium nitride (GaN) under high pressure. They calculated the bulk modulus, compression ratio, lattice constant, and phonon frequency spectrum of GaN under high pressure to 40 GPa using three B–M and modified Lennard–Jones EOSs. The agreements of their results for the phonon frequency spectrum that were obtained using B–M EOS with experimental data were better than those obtained from modified Lennard–Jones EOS [28].

Equations of state EOSs serve as tests for the calculation of the electronic structure of different properties of metals as well as they are used as scales for high pressure [29]. Most of the experiments of pressure–volume (PV) measurements on solids under high pressure were executed using almost small pressure ranges. As it is known, all EOSs can be fitted to experimental PV data taking into consideration the elastic constants, i.e., the isothermal bulk modulus (B_0), and its pressure derivatives (B_0') [30, 31]. There are many methods to determine those elastic constants, like the PV relations and measurement of the velocity of the acoustic waves, besides the dispersion curves of the branches of acoustic phonon [32]. When those experimental data are fitted with any EOS such as B–M, then the isothermal bulk modulus B_0 and its first pressure derivative at atmospheric pressure and ambient temperature B_0' can be extracted. Those parameters will be useful in the EOS to obtain different important parameters concerning the solid materials under pressure, and they could be helpful for the calculations that can be extrapolated toward higher pressure ranges when theoretical aspects are taken into consideration [29, 33].

The aim of this work is to study the variation of the isothermal bulk modulus, the pressure derivative of bulk modulus, and the volumetric thermal expansion coefficient as a function of high hydrostatic pressure for nine metallic elements of different atomic weights. It is worth to mention that all data concerning the pressure versus relative volume of all nine elements used in this work were taken from the experimental works published by other researchers. Those elements were namely, potassium (K) [34], aluminum (Al)

[35], beryllium (Be) [8], gold (Au) [36], copper (Cu) [37], tantalum (Ta) [18], cobalt (Co) [12], molybdenum (Mo) [38], and tungsten (W) [36]. The data of those researchers were either taken from tables or as graphics points of the figures mentioned within their researches. The experimental data taken from the graphs were done with the aid of GRABIT software that works with MATLAB.

2. Theoretical Background

Any equation that relates the pressure (P), specific volume (V), and temperature (T) of a material in the thermal equilibrium state is called the equation of state EOS. The simplest EOS is that of an ideal gas. There are many EOSs describing the state of solid materials under high pressure such as Murnaghan, Birch, Birch–Murnaghan, Vinet, modified Leanard–Jones EOSs, and others.

2.1. Birch–Murnaghan (B–M) EOS. The third order B–M EOS is given as follows [39]:

$$P=\frac{3B_0}{2}\left[\left(\frac{V}{V_0}\right)^{\frac{-7}{3}}-\left(\frac{V}{V_0}\right)^{\frac{-5}{3}}\right]\left[1+\frac{3}{4}(B_0'-4)\left(\left(\frac{V}{V_0}\right)^{\frac{-2}{3}}-1\right)\right], \tag{1}$$

where B_0 is the isothermal bulk modulus at atmospheric pressure and ambient temperature, B_0' is the first pressure derivative of the bulk modulus at ambient temperature, V_0 and V are the volumes at atmospheric pressure and pressure (P), respectively. It is worth to mention that the above equation was derived on the basis of Eulerian finite strain theory which is useful to describe solids under high pressure applications [40]. This equation is the most widely used by researchers [41].

2.2. Isothermal Bulk Modulus and Its Derivatives. Bulk modulus can be defined as the ability of a material to bear the change in its volume when pressure is applied to all sides. It can be considered one of the fundamental mechanical properties of structural solids which can be deduced through the measurement of the unit cell volume [41]. The isothermal bulk modulus B_T can be calculated from the following equation:

$$B_T=-V\left(\frac{\partial P}{\partial V}\right)_T. \tag{2}$$

Equation (2) implies that the isothermal bulk modulus is given by the ratio of the increase in the applied pressure divided by the relative deformation. Before deriving the pressure in Equation (1) with respect to the volume and substituting it in Equation (2), it is necessary to simplify Equation (1) to be easier for differentiation. So, the pressure (P) in Equation (1) can be rewritten in the following simple form:

$$\begin{aligned}P=&\frac{1}{2}B_0\left[3\left(\frac{V}{V_0}\right)^{-\frac{7}{3}}-3\left(\frac{V}{V_0}\right)^{-\frac{5}{3}}\right]\\&+\frac{3}{8}B_0(B_0'-4)\left[3\left(\frac{V}{V_0}\right)^{-3}-6\left(\frac{V}{V_0}\right)^{-\frac{7}{3}}+3\left(\frac{V}{V_0}\right)^{-\frac{5}{3}}\right].\end{aligned} \tag{3}$$

By keeping the temperature constant and differentiating the pressure in Equation (3) with respect to the volume, then,

$$\begin{aligned}\left(\frac{dP}{dV}\right)_T=&\frac{-1}{2}\frac{B_0}{V}\left[7\left(\frac{V}{V_0}\right)^{-\frac{7}{3}}-5\left(\frac{V}{V_0}\right)^{-\frac{5}{3}}\right]\\&-\frac{3}{8}\frac{B_0}{V}(B_0'-4)\left[9\left(\frac{V}{V_0}\right)^{-3}-14\left(\frac{V}{V_0}\right)^{-\frac{7}{3}}+5\left(\frac{V}{V_0}\right)^{-\frac{5}{3}}\right].\end{aligned} \tag{4}$$

Substituting Equation (4) into Equation (2), the isothermal bulk modulus under high pressure is expressed as follows:

$$\begin{aligned}B_T=&\frac{1}{2}B_0\left[7\left(\frac{V}{V_0}\right)^{\frac{-7}{3}}-5\left(\frac{V}{V_0}\right)^{\frac{-5}{3}}\right]\\&+\frac{3}{8}B_0(B_0'-4)\left[9\left(\frac{V}{V_0}\right)^{-3}-14\left(\frac{V}{V_0}\right)^{\frac{-7}{3}}+5\left(\frac{V}{V_0}\right)^{\frac{-5}{3}}\right].\end{aligned} \tag{5}$$

Most of the EOSs, including B–M finite strain EOS have been widely used for the investigation of high-pressure properties of solid materials. Equations (1) and (5) show that both of the bulk modulus and pressure increase as the relative volume (V/V_0) decreases and that at extreme compression ($V=0$) both of P and B_T become infinite [42]. Values of the first pressure derivative of the bulk modulus at a given temperature and atmospheric pressure have been found to decrease with the increase of pressure and then become almost constant at extreme compression ($V=0$). The pressure derivative of the bulk modulus can be found from the derivation of the isothermal bulk modulus with respect to the pressure as follows:

$$B'=\left(\frac{dB}{dP}\right)_T=\left(\frac{dB}{dV}\right)_T\left(\frac{dV}{dP}\right)_T, \tag{6}$$

which can be written as follows:

$$B'=\frac{-V}{B_T}\left(\frac{dB}{dV}\right)_T. \tag{7}$$

Now the $(dB/dV)_T$ must be found first,

$$\begin{aligned}\left(\frac{dB}{dV}\right)_T=&\frac{-B_0}{8V}\left[(B_0'-4)\left\{81\left(\frac{V}{V_0}\right)^{-3}-98\left(\frac{V}{V_0}\right)^{-\frac{7}{3}}\right.\right.\\&\left.\left.+25\left(\frac{V}{V_0}\right)^{-\frac{5}{3}}\right\}+\frac{4}{3}\left\{49\left(\frac{V}{V_0}\right)^{-\frac{7}{3}}-25\left(\frac{V}{V_0}\right)^{-\frac{5}{3}}\right\}\right],\end{aligned} \tag{8}$$

and by substituting for $(dB/dV)_T$ into Equation (5), the pressure derivative of the bulk modulus with respect to the pressure can be written as follows:

$$B' = \frac{B_0}{8B_T}\left[(B_0' - 4)\left\{81\left(\frac{V}{V_0}\right)^{-3} - 98\left(\frac{V}{V_0}\right)^{-\frac{7}{3}} + 25\left(\frac{V}{V_0}\right)^{-\frac{5}{3}}\right\} + \frac{4}{3}\left\{49\left(\frac{V}{V_0}\right)^{-\frac{7}{3}} - 25\left(\frac{V}{V_0}\right)^{-\frac{5}{3}}\right\}\right]. \tag{9}$$

The derivative of the bulk modulus with respect to pressure B' plays an important role in determining thermoplastic parameters of solids at high compression [2]. Making use of Equation (9) together with Equations (1) and (4), the derivative of the bulk modulus with respect to pressure B' can be obtained as a function of the pressure (P).

2.3. Volumetric Thermal Expansion Coefficient. Since the product of the volumetric thermal expansion coefficient (α) and the isothermal bulk modulus (B_T) is constant and holds for all solids. Thus,

$$\alpha.B_T = \text{Constant}. \tag{10}$$

Shanker and Kumar [43] showed the following:

$$\frac{\alpha}{\alpha_0} = \left(\frac{V}{V_0}\right)^{\delta_T}, \tag{11}$$

where α_0 is the volumetric expansion coefficient at atmosphere pressure ($P = 0$) and δ_T is the isothermal Anderson parameter. Moreover, they showed the following:

$$\frac{B_T}{B_0} = \left(\frac{V}{V_0}\right)^{-\delta_T}, \tag{12}$$

from which one can write the following:

$$\left(\frac{B_T}{B_0}\right)\left(\frac{\alpha}{\alpha_0}\right) = 1, \tag{13}$$

or

$\alpha.B_T = \alpha_0 B_0$, from which one can write the following:

$$\alpha = \frac{\alpha_0}{\left(\frac{B_T}{B_0}\right)}. \tag{14}$$

By combining Equations (4) and (14), the volumetric thermal expansion coefficient can be written as follows:

$$\alpha = 2\alpha_0\left[\left[7\left(\frac{V}{V_0}\right)^{\frac{-7}{3}} - 5\left(\frac{V}{V_0}\right)^{\frac{-5}{3}}\right] + \frac{4}{3}(B_0' - 4)\left[9\left(\frac{V}{V_0}\right)^{-3} - 14\left(\frac{V}{V_0}\right)^{\frac{-7}{3}} + 5\left(\frac{V}{V_0}\right)^{\frac{-5}{3}}\right]\right]^{-1}. \tag{15}$$

It is worth to mention here that the equations for the bulk modulus, its first pressure derivative and that of the volumetric bulk thermal expansion coefficient are not expressed directly in terms of pressure, but they were expressed instead in terms of the relative volume (V/V_0). Then, by making use of Equations (1), (4), and (15), and knowing the values of α_0, the volumetric thermal expansion coefficient α of the given solid elements can be calculated as a function pressure (P).

3. Results and Discussion

The experimental P–V data of all nine elements of the researchers that were mentioned in the introduction of this work were fitted to the B-EOS given by Equation (1). The experimental method used by those researchers for hcp-beryllium, fcc-gold, hcp-cobalt, bcc-tantalum, bcc-molybdenum, and bcc-tungsten was DAC.

The experimental method used for bcc potassium was a pressure vessel and that used for fcc aluminum was tungsten carbide opposed anvil. Values of B_0 and B_0' were extracted for each element and they were tabulated in Table 1. The P–V isotherms of those elements were plotted in the figures, i.e., Figures 1–5. The P–V isotherm of potassium is plotted within Figure 1 using Equation (1) after substitution of its B_0 and B_0' from Table 1. Moreover, the experimental data for potassium done by Kim and Ruoff [34] were plotted in Figure 1. Other experimental data of Lundegaard et al. [11] and Winzenick et al. [9] were plotted with the same potassium isotherm for comparison. Data of Winzenick et al. [9] are generally in good agreement with the plotted potassium isotherm and the data [11] also seem in good agreement with it at low pressures, i.e., up to nearly 2.5 GPa, but as the pressure exceeds 2.5 GPa, differences between them increase gradually.

This is attributed to B–M EOS that was driven on the basis of Eulerian finite strain, and its description of the solid material compression under high pressure is not adequate, as mentioned by Alkammash [67]. The isotherm of aluminum is also plotted in Figure 1, making use of B–M EOS given by Equation (1) with its values of B_0 and B_0' from Table 1. Moreover, the experimental data of Syassen and Holzapfel [35] were plotted with the isotherm. The values of B_0 and B_0' extracted in this work were very close to those deduced by Syassen and Holzapfel [35], and the little differences may be due to the errors in picking the points from Figure 1 of Syassen and Holzapfel [35]. Also, the experimental data of Dewaele et al. [36] and Ming and Manghnani [60], as well as those of Thomas [48], were plotted within the same figure for comparison. The data of Dewaele et al. [36] and those of Vaboya and Kennedy [60] seem to be in good agreement

Table 1: Bulk modulus and its first pressure derivative from experimental data fitted to Birch–Murnaghan EOS.

Element	Experimental work	B_0 (Gpa)	$B_0{}'$	This work
Potassium	[34]	4.307 ± 0.153	3.207 ± 0.059	Data fitted to B–M EOS in this work
	[44]	3.44	3.85	
	[45]	3.09	3.98	
	[46]	3.395	2.971	
Aluminum	[35]	73.37 ± 0.966	4.123 ± 0.248	Data fitted to B–M EOS in this work
	[47]	73	4.45	
	[48]	71.7 ± 3.6	4.42	
	[49]	72.9 ± 0.3	4.42	
Beryllium	[8]	101.428 ± 2.157	3.515 ± 0.055	Data fitted to B–M EOS in this work
	[50]	111	4.6	
	[51]	91	3.4	
	[52]	121	3.4	
Gold	[36]	171.74 ± 5.09	5.526 ± 0.047	Data fitted to B–M EOS in this work
	[53]	167.2	5.21	
	[48]	163.5 ± 8.3	5.21	
	[54]	166.4	7.3	
Copper	[37]	183.31 ± 6.802	3.807 ± 0.261	Data fitted to B–M EOS in this work
	[54]	137.4	5.52	
	[53]	131.4	5.44	
	[17]	120.7 ± 2.1	5.3 ± 0.2	
Cobalt	[12]	209.345 ± 5.145	3.244 ± 0.185	Data fitted to B–M EOS in this work
	[55]	196.5	4.007	
	[56]	203 ± 2	3.6 ± 0.1	
	[57]	199	3.6	
Tantalum	[18]	194.215 ± 5.05	3.453 ± 0.108	Data fitted to B–M EOS in this work
	[58]	194	3.74	
	[59]	194	3.83	
	[60]	206	2.76	
Molybdenum	[38]	249.55 ± 2.786	3.86 ± 0.086	Data fitted to B–M EOS in this work
	[61]	267	4.46	
	[62]	260	4.21	
	[14]	255	4.25	
	[63]	260	4.32	
	[64]	260.79	4.35	
Tungsten	[36]	279.626 ± 3.132	6.265 ± 0.351	Data fitted to B–M EOS in this work
	[16]	308	4.20	
	[65]	304	4.1	
	[66]	312	3.68	

with the fitted data, while those of Ming et al. [48] have little deviation from the fitted data.

Experimental P–V data of Nakano et al. [8] for Be were fitted to the B–M EOS, and those data, together with the fitted curve, were drawn in Figure 2. Be has hcp (phase II) at atmospheric pressure up to 1,523 k; its unit cell has the dimensions of $a = 0.2286$ nm, $c = 0.3584$ nm, and $c/a = 1.56$ [8]. There is no practical evidence for phase transformation of Beryllium up to 171 GPa [8]. The elastic constants that were extracted from the fitting were $B_0 = 101.428 \pm 2.157$ GPa, $B_0' = 3.515 \pm 0.055$. These are in good agreement with those that were found by other researchers that were tabulated in Table 1. In order to compare the above fitted data with the data published by other authors, the experimental P–V data of Ming and Manghnani [68] and Velisavljevic et al. [6], were plotted in the same figure. It seems that Velisavljevic et al. [6] data are in good agreement with those of Nakano et al. [8], while the data of Ming and Manghnani [68] are in good agreement with Nakano et al. [8] data up to nearly 30 GPa but after that, it is clear that deviation between them began increasing until 170 GPa. This deviation can also be justified by the reason mentioned by Alkammash [67]. Gold isotherm was also plotted within Figure 2 using the extracted B_0 and B_0' after their substitution in Equation (1). Values of B_0 and B_0' were in good agreement with those found by Heinz and

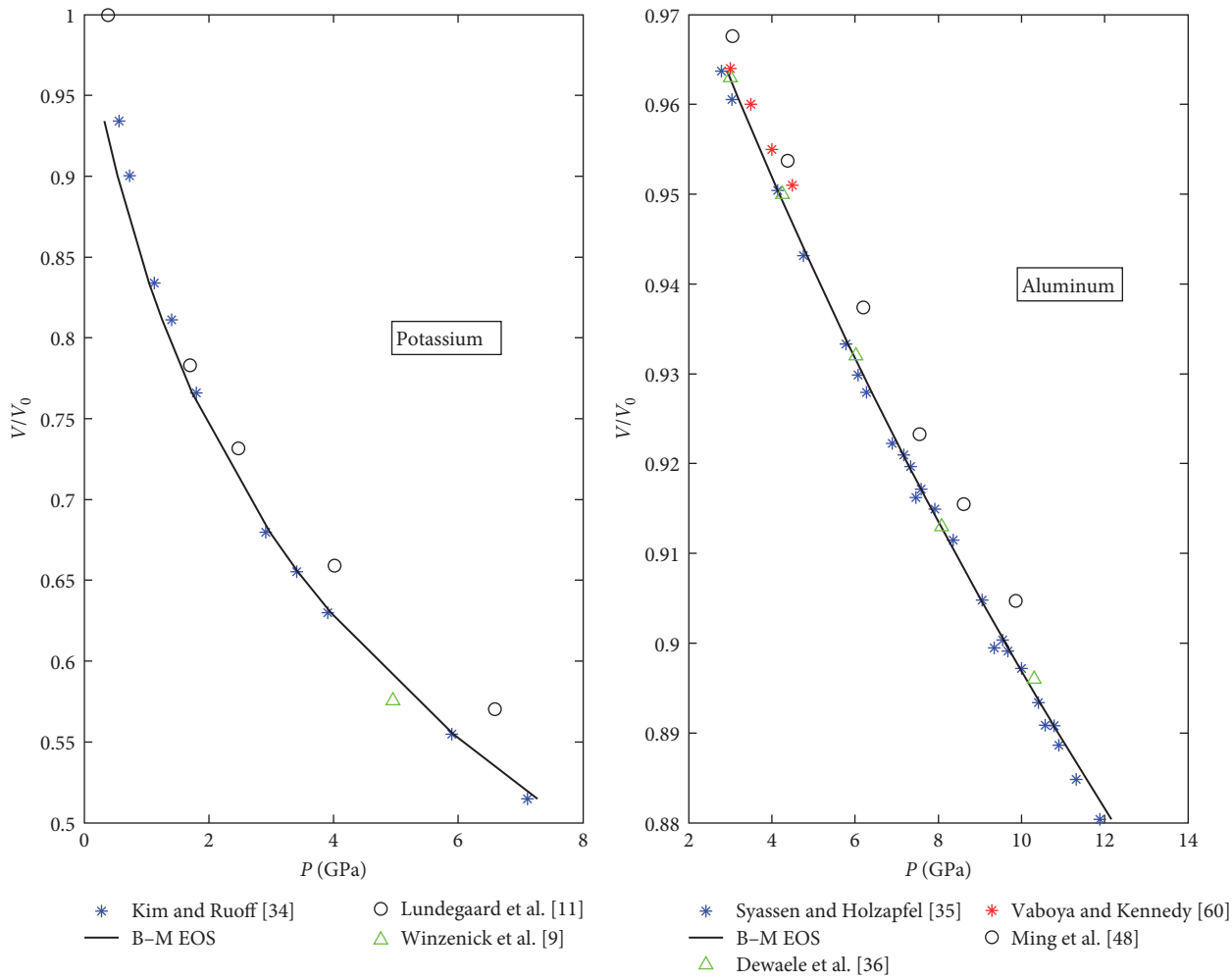

FIGURE 1: Pressure–volume experimental data of Kim and Ruoff [34] for potassium (K) and Syassen and Holzapfel [35] for aluminum (Al) fitted to B–M EOS (solid line) and compared with other researchers' experimental data.

Jeanloz [69] that are $B_0 = 167$ GPa and $B_0' = 5.5$. The P–V experimental data of Ming et al. [48], Takemura and Dewaele [70], Heinz and Jeanloz [69], and Bridgman [71] for the Gold were also plotted on the same figure. They show good agreement with the fitted data.

The P–V isotherm of Cu was plotted in Figure 3 using Equation (1) and by taking the values of B_0 and B_0' from Table 1. Experimental data from Mao et al. [37] that were fitted to B–M EOS were plotted with them in Figure 2. The experimental P–V data of Cu of researchers Dewaele et al. [36] and Xu et al. [72] were also plotted on the same figure for comparison. Xu et al. [72] data showed almost good agreement with the fitted data, while Dewaele et al. [36] data showed some deviation from B–M EOS. Also, this deviation increases as the pressure increases. This can also be attributed to the reason that B–M EQS cannot describe adequately the solid under the compression at very high pressures, as mentioned above. At 300 k and 0.1 MPa, Ta has a bcc structure, and its lattice constant and melting point are $a = 0.3297$ nm and 3,247°C, respectively [73]. According to Söderlind and Moriarty [74], it was shown theoretically that the Ta bcc lattice structure remains stable up to 1 TPa. By fitting the P–V experimental data of Cynn and Yoo [18] for Ta to the B–M EOS, it was shown that $B_0 = 194.2$ GPa and $B_0' = 3.453$ which are in good agreement with those values that were got by ultrasonic measurements. Using theoretical calculations, it was estimated that the value of B_0 of Ta to be 203–211 GPa at 0 k [18]. Figure 3 shows the experimental data of Xu et al. [72] and Litasov et al. [61] that were plotted with the Ta-fitted data for comparison. There was good agreement between the experimental data and B–M EOS at low pressure and again deviation between them starts as pressure increases until it exceeds 50 GPa.

For Cobalt (Co) elements, the experimental P–V data were taken from Fujihisa and Takemura [12], as mentioned earlier. Co has hcp and fcc phases. In this work, only the hcp phase data of cobalt were taken into consideration and were fitted to B–M EOS, and the bulk modulus and its first pressure derivative at ambient temperature were found to be $B_0 = 209.345 \pm 5.145$ GPa and $B_0' = 3.244 \pm 0.185$, respectively. The above hcp phase experimental data, together with co isotherm, were plotted in Figure 4, and the experimental data of Yoo et al. [56] and those of Ono [57] were plotted in the same figure for comparison. From Figure 4, it

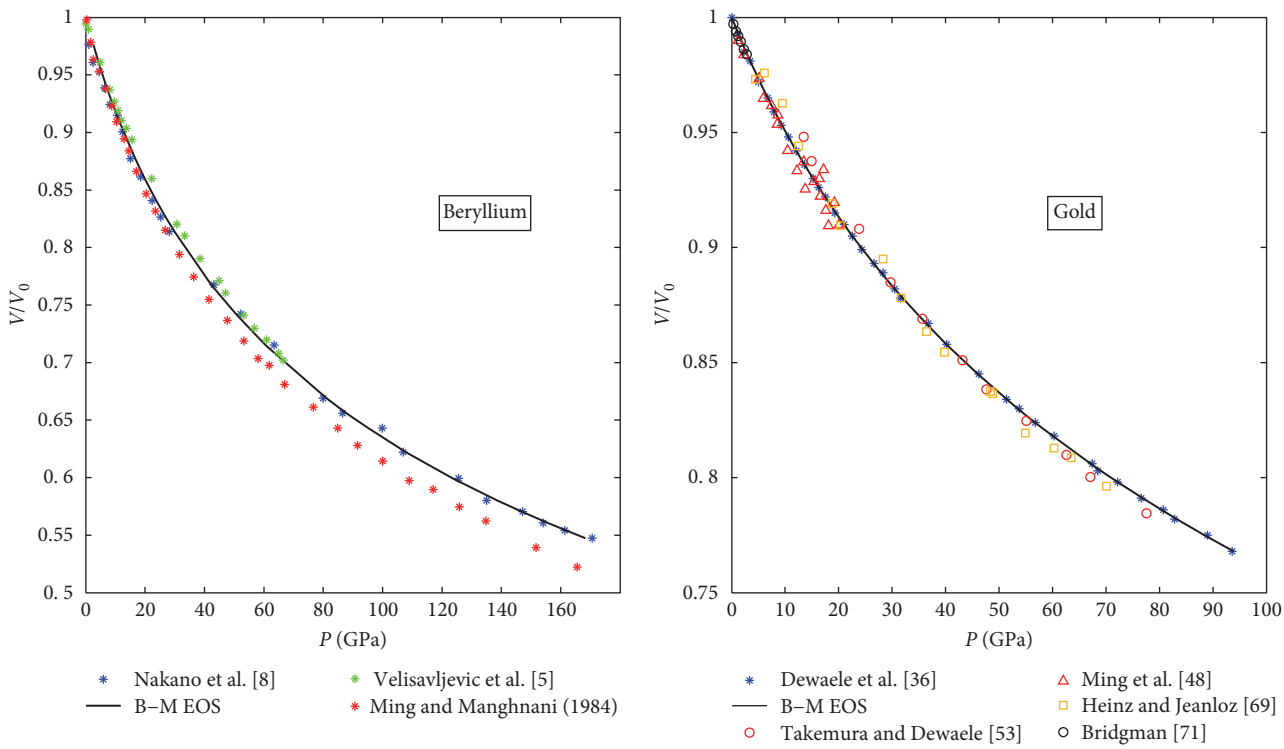

Figure 2: Pressure–volume experimental data of Nakano et al. [8] for beryllium (Be) Dewaele et al. [36] for gold (Au), fitted to B–M EOS (solid line) and compared with other researchers.

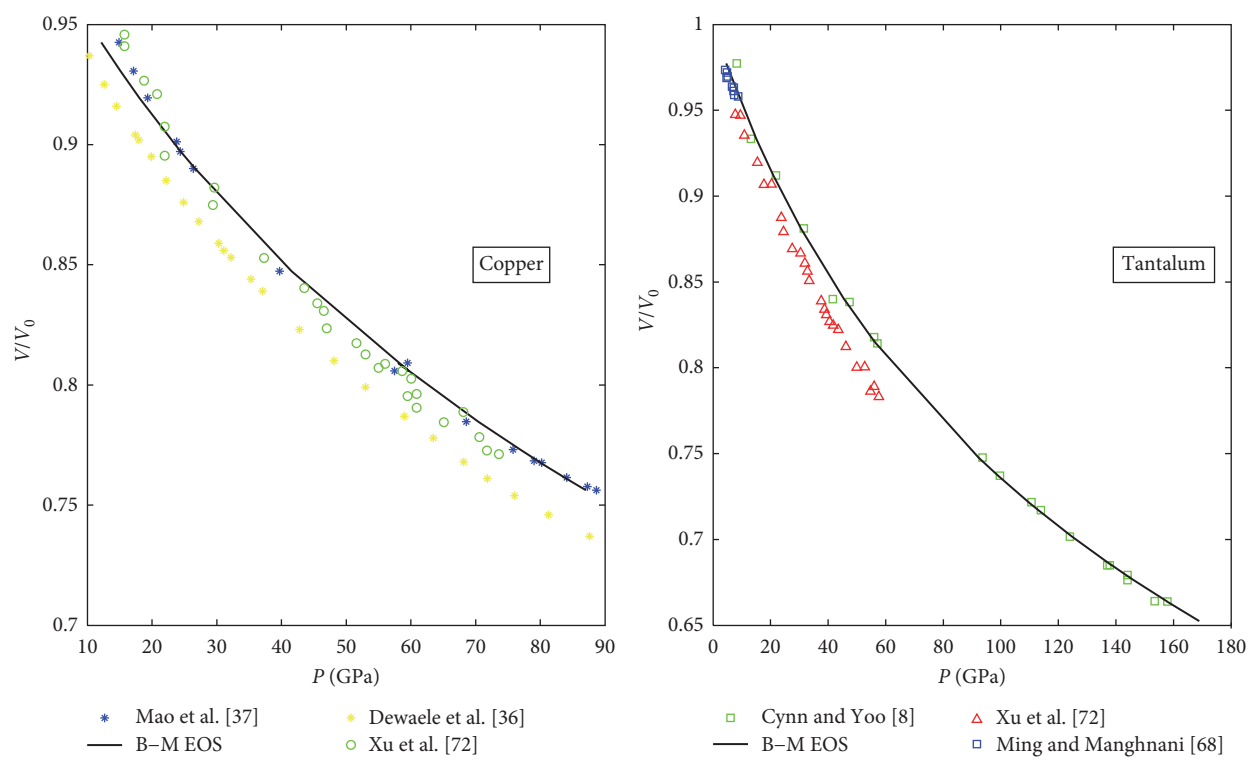

Figure 3: Pressure–volume experimental data of Mao et al. [37] for copper (Cu) and Cynn and Yoo [18] for tantalum (Ta), fitted to B–M EOS (solid line) and compared with other researchers' experimental data.

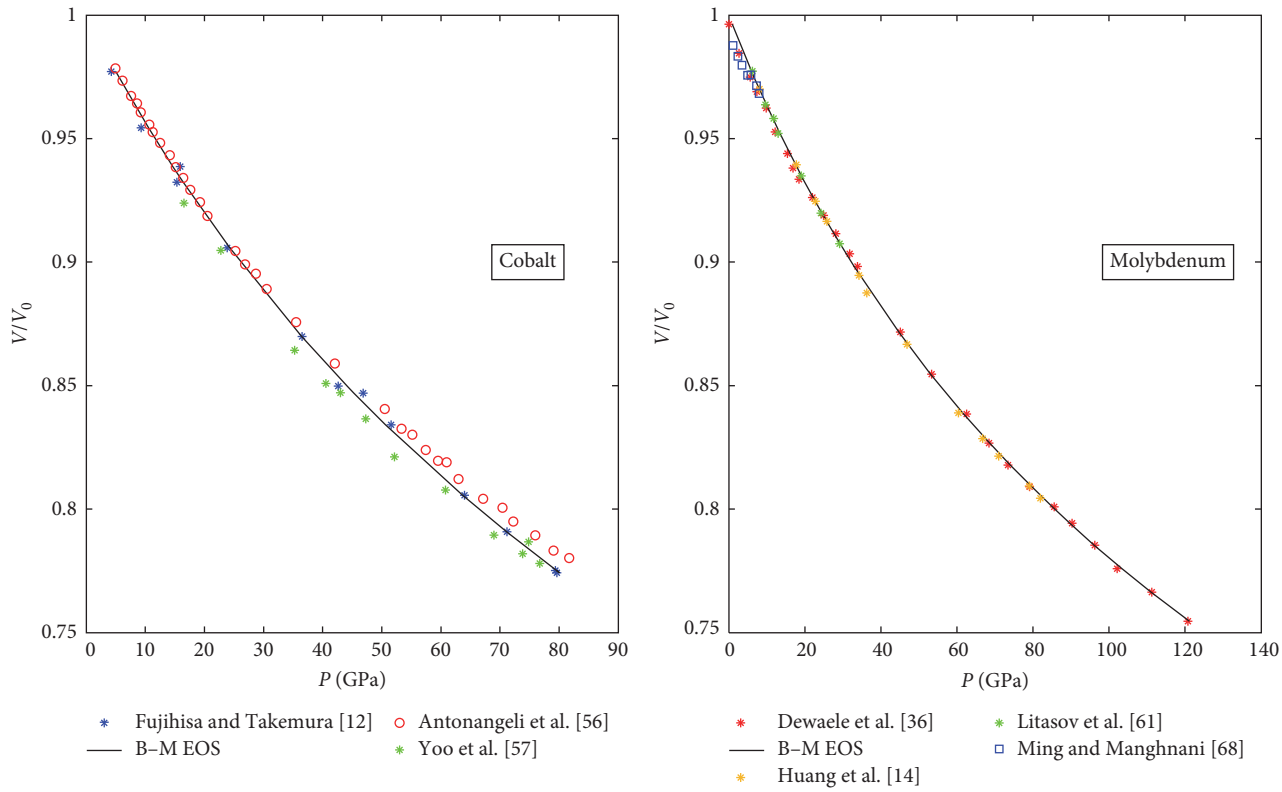

FIGURE 4: Pressure–volume experimental data of Fujihisa and Takemura [12] for cobalt (Co) and Dewaele et al. [38] for molybdenum (Mo), fitted to B–M EOS (solid line) and compared with other researchers' experimental data.

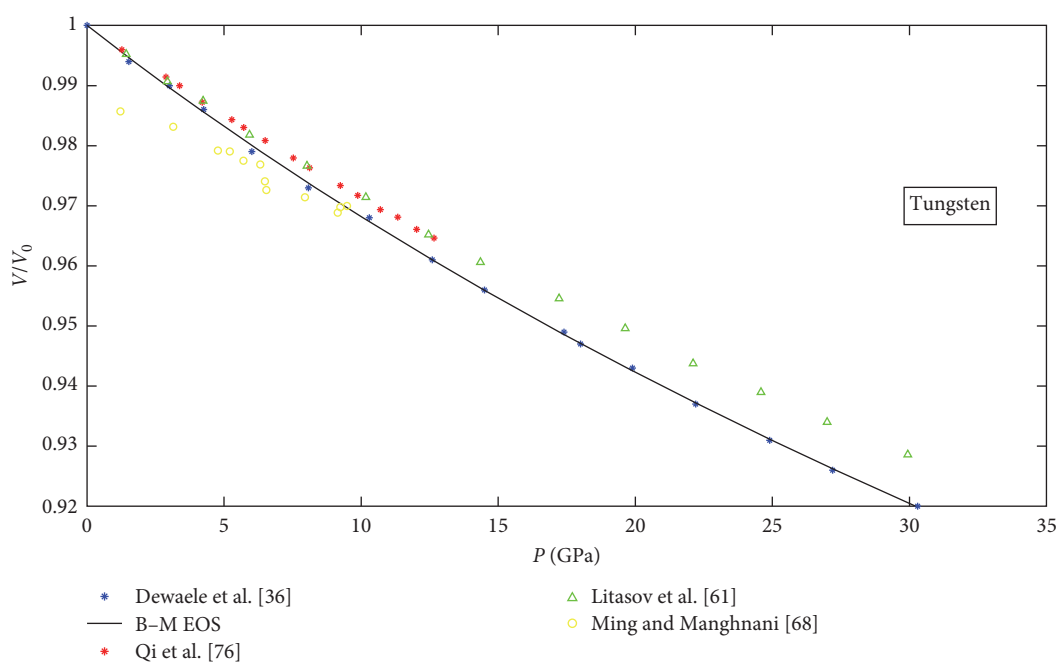

FIGURE 5: Pressure–volume experimental data of Dewaele et al. [36] for tungsten (W), fitted to B–M EOS (solid line) and compared with other researchers' experimental data.

is obvious that almost good agreement can be seen between the fitted data to B–M, EOS, and Yoo. The elastic parameters of the molybdenum (Mo), $B_0 = 249.55 \pm 2.786$ GPa and $B_0' = 3.86 \pm 0.086$ were extracted through the fitting of the experimental P–V data of Dewaele et al. [38] to B–M EOS and were used to plot the Mo isotherm in Figure 4. Moreover, the P–V experimental data of Huang et al. [14], Litasov et al. [61], and Sokolova et al. [62] were plotted in the same

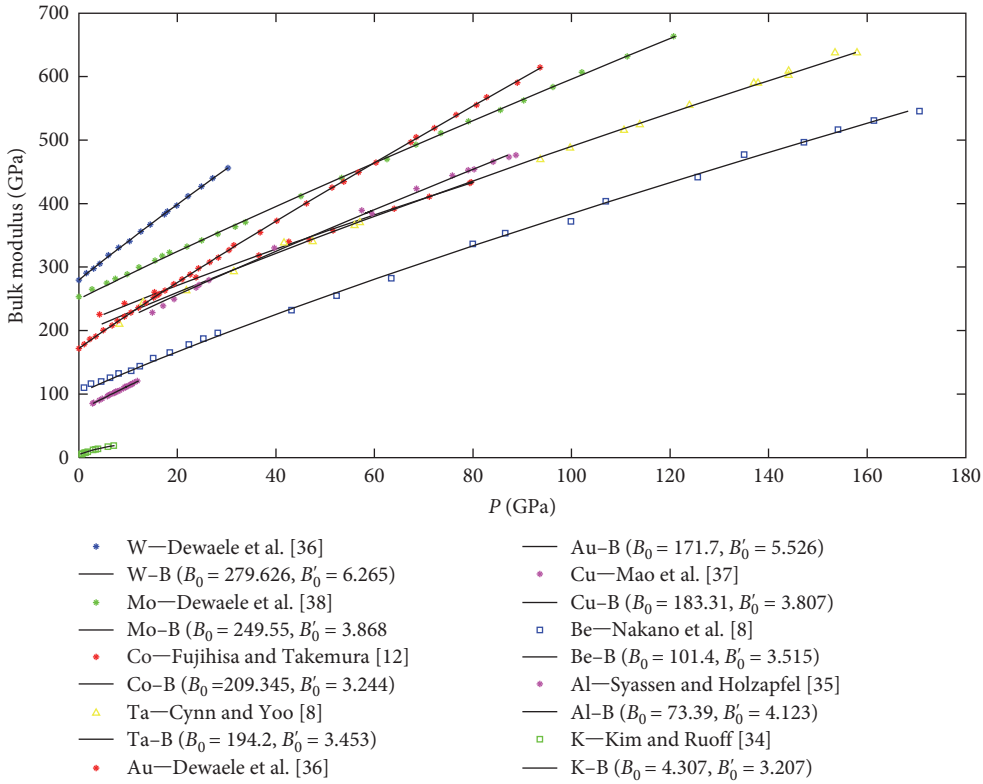

Figure 6: Variation of isothermal bulk modulus with the applied pressure for all nine elements. The solid lines are the calculated bulk moduli using Equation (3), while the data points the bulk moduli calculated by Equation (3) based on fitted experimental data of pressure–volume.

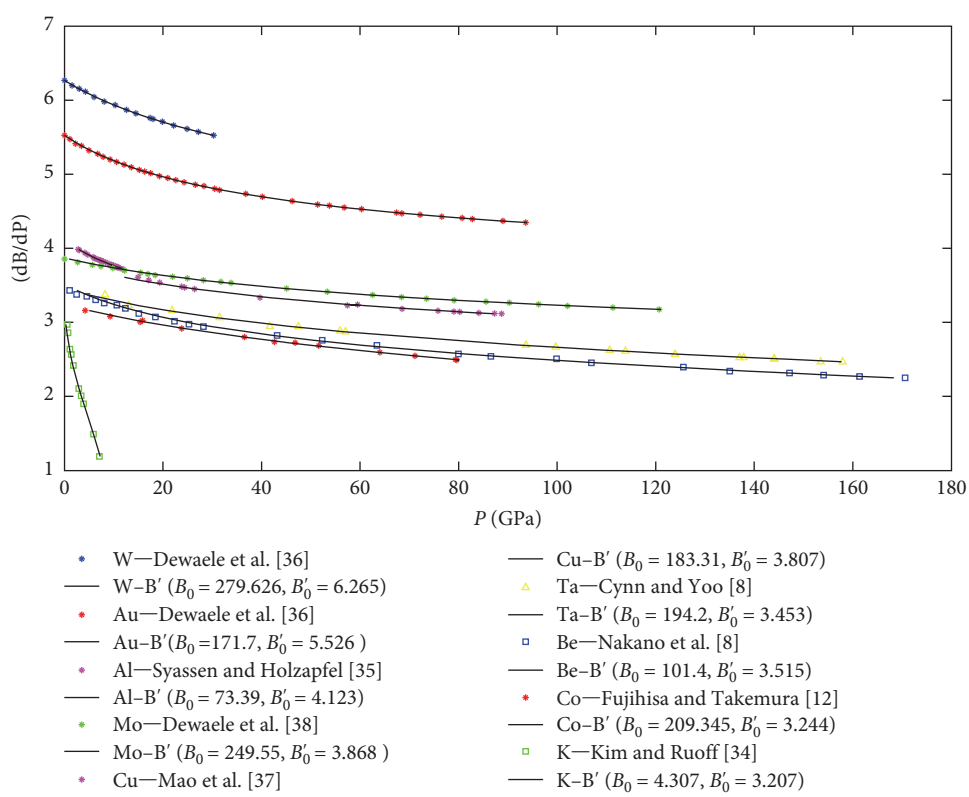

Figure 7: Pressure derivative of bulk modulus at atmospheric pressure ($P = 0$) and ambient temperature as a function of pressure. All experimental P–V data used in the calculation are mentioned in the figure legend.

Table 2: Values of thermal expansion coefficient.

Element	$\alpha_v \times 10^{-6}$ per k	Reference
Potassium	249	[77]
Aluminum	75	[78]
Beryllium	34.8	[79]
Gold	41.7	[77]
Copper	49.8	[78]
Tantalum	19.8	[77]
Cobalt	37.2	[77]
Molybdenum	15.6	[77]
Tungsten	13.8	[77]

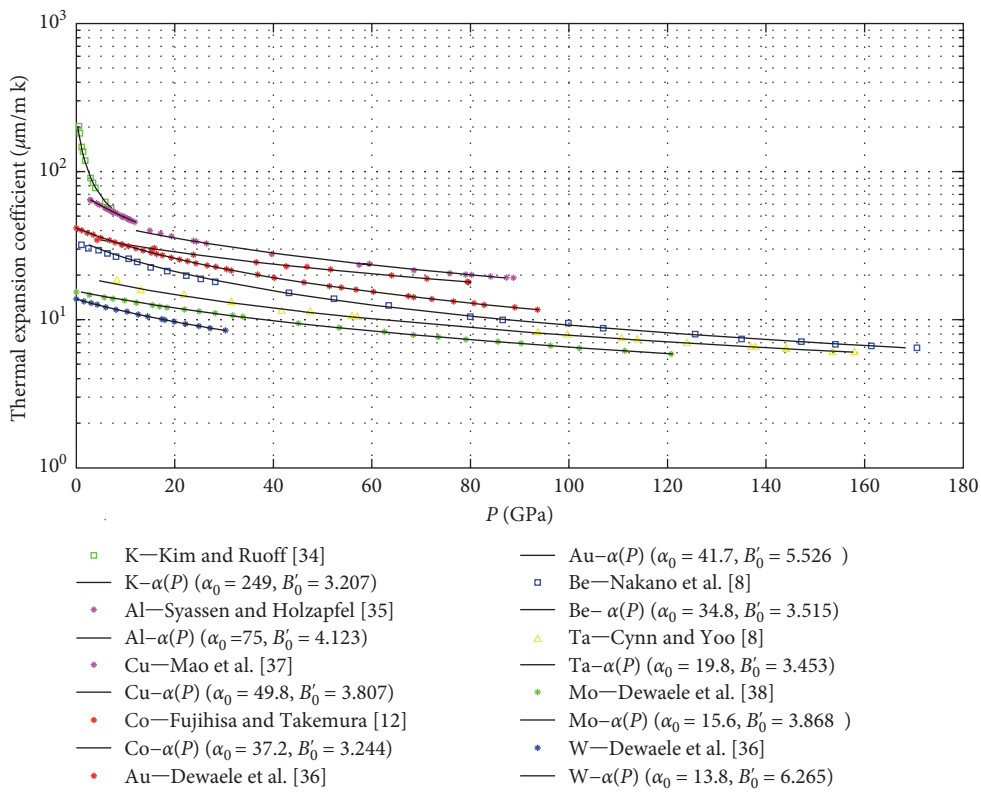

Figure 8: Variation of volumetric thermal expansion coefficient of the metallic elements as a function of pressure. All experimental P–V data used in the calculation are mentioned in the figure legend.

figure for the sake of comparison. Good agreement was shown between those data with the fitted data of Dewaele et al. [38], as shown in Figure 4.

The P–V experimental data of Dewaele et al. [36] for tungsten were fitted to B–M EOS, and the isothermal bulk modulus at atmospheric pressure and its first pressure derivative was found to be $B_0 = 279.626 \pm 3.132$ GPa and $B_0' = 6.265 \pm 0.51$. Pressures between 200 and 300 GPa have been used when the Tungsten has been studied under hydrostatic compression, and the crystallographic structures were found to be stable according to the expectation of the electronic transfer of s to d [75]. The experimental data of tungsten of Litasov et al. [61], Dubrovinsky et al. [16], and Wilson [76] were plotted together with the fitted data of a B–M EOS in Figure 3 for comparison. The agreement is almost good, especially at low pressures.

It is mentioned by many researchers that the bulk modulus of solid materials increases linearly with increasing the applied pressure [32, 41]. Equations (1) and (4) were used to plot the variation of bulk modulus values as a function of the applied pressure for the selected nine elements after substitution of the values of B_0 and B_0' that were found from the fitting in Figure 6. It can be seen from the figure that the variation of the bulk modulus with the pressure for all nine elements is almost linear. It is worth to mention that the variation of the bulk modulus with the applied pressure is also given by the equation $B = B_0 + B_0' P$ and that the higher orders of nonlinear

terms B_0'', B_0''' were neglected and this is known as Murnaghan approximation [43]. This is why some of the curves in Figure 6 show a slight tendency toward curvature shape. The differences in the slopes of the lines in Figure 6 were attributed to the differences in the values of the first pressure derivatives at atmospheric pressure B_0' of the elements that are shown in Table 1. The highest slope is for tungsten, which has the highest B_0' value (6.265), while the lowest slope is for potassium, which has the lowest B_0' value is 3.207.

The first pressure derivatives of the bulk modulus $B'(P)$ as a function of pressure for all nine elements were determined from Equations (1) and (9) and plotted versus pressure in Figure 7. It can be seen from this figure that the $B'(P)$ of most of the selected elements decreases slightly with increasing pressure. This can be attributed to the fact that most of those elements, like W, Au, Mo, Al, Co, Ta, Cu, and Be, relatively possess high values of bulk modulus, as shown in Table 1. Therefore, $B'(P)$ seems to decrease slowly with pressure and tends to be constant. Thus, the total variation from the initial values of B_0' seems to be not too much. On the other hand, the last selected element in this work, which is potassium, has a very low bulk modulus, as can be seen from Table 1. It is clear from Figure 7 that the $B'(P)$ for potassium decreases rapidly with increasing pressure. This can be interpreted that potassium is a relatively soft material compared to other selected metallic elements and has small stiffness, so the pressure rate of change of its bulk modulus decreases with increasing pressure.

With a few exceptions, all materials expand when heated. However, the extent of expansion per degree change in temperature is different for different materials. Equation (15) is used to determine the volumetric thermal expansion coefficient $\alpha(P)$ of all the nine elements. Values of thermal expansion coefficients at atmospheric pressure α_o shown in Table 2 for those elements together with the first derivative of the bulk modulus at atmospheric pressure B_0' were substituted in the equation. Figure 8 shows the variation of $\alpha(P)$ with the applied pressure. It is clear from the figure that $\alpha(P)$ decreases with increasing pressure. Thermal expansion is reduced by the effect of large pressures that cause decoupling heat from mechanical work.

4. Conclusion

The third-order B–M EOS was used in this work, and the isothermal bulk modulus, its first pressure derivative and the volumetric thermal expansion coefficient equations were derived based on this equation. The isothermal P–V diagrams for nine metallic elements was plotted based on the B–M EOS mentioned above by making use of their B_0 and B_0' values. Values of B_0 and B_0' were extracted by fitting the experimental P–V data of those metallic elements executed under high hydrostatic compression by different researchers to the B–M EOS and compared with the published values and showed good agreement. The variation of the isothermal bulk modulus with the applied pressure for the nine metallic elements were studied. It was shown that as the applied pressures increase, the isothermal bulk modulus also increases. The first derivative of the bulk modulus with respect to the pressure for the nine metals seems to decrease slowly as the pressure increases. The variation of the volumetric thermal expansion coefficient of those elements with the applied pressure was studied in this research. It was shown that as the applied pressure increases, the volumetric thermal expansion coefficient decreases.

Data Availability

The data used to support the findings of this study are included within the article.

Conflicts of Interest

The authors declare no conflicts of interest.

Acknowledgments

The authors want to acknowledge Prof. Matteo Alvaro, Professor of Mineralogy at the University of Pavia, Italy and Dr. Nawzat S. Saadi from the College of Science, University of Duhok, Iraq for the scientific advisory effort during the completion of this work. This research was supported by the University of Duhok, Iraq and the University of Mosul, Iraq.

References

[1] H. K. Hieu and N. N. Ha, "High pressure melting curves of silver, gold and copper," *AIP Advances*, vol. 3, no. 11, pp. 0–9, 2013.

[2] F. D. Stacey, "High pressure equations of state and planetary interiors," *Reports on Progress in Physics*, vol. 68, no. 2, Article ID 341, 2005.

[3] A. Dewaele and P. Loubeyre, "Mechanical properties of tantalum under high pressure," *Physical Review B*, vol. 72, no. 13, Article ID 134106, 2005.

[4] P. W. Bridgman, "The effect of pressure on the tensile properties of several metals and other materials," *Journal of Applied Physics*, vol. 24, no. 5, pp. 560–570, 1953.

[5] E. Güler and M. Güler, "Geometry optimization calculations for the elasticity of gold at high pressure," *Advances in Materials Science and Engineering*, vol. 2013, Article ID 525673, 5 pages, 2013.

[6] N. Velisavljevic, G. N. Chesnut, Y. K. Vohra, S. T. Weir, V. Malba, and J. Akella, "Structural and electrical properties of beryllium metal to 66 GPa studied using designer diamond anvils," *Physical Review B*, vol. 65, no. 17, Article ID 172107, 2002.

[7] W. J. Evans, M. J. Lipp, H. Cynn et al., "X-ray diffraction and raman studies of beryllium: static and elastic properties at high pressures," *Physical Review B - Condensed Matter and Materials Physics*, vol. 72, no. 9, pp. 1–6, 2005.

[8] K. Nakano, Y. Akahama, and H. Kawamura, "X-ray diffraction study of Be to megabar pressure," *Journal of Physics: Condensed Matter*, vol. 14, no. 44, Article ID 10569, 2002.

[9] M. Winzenick, V. Vijayakumar, and W. B. Holzapfel, "High-pressure X-ray diffraction on potassium and rubidium up to 50 GPa," *Physical Review B*, vol. 50, no. 17, pp. 12381–12385, 1994.

[10] V. F. Degtyareva, "Potassium under pressure: electronic origin of complex structures," *Solid State Sciences*, vol. 36, no. Figure 1, pp. 62–72, 2014.

[11] L. F. Lundegaard, G. W. Stinton, M. Zelazny et al., "Observation of a reentrant phase transition in incommensurate potassium," *Physical Review B*, vol. 88, no. 5, Article ID 054106, 2013.

[12] H. Fujihisa and K. Takemura, "Equation of state of cobalt up to 79 GPa," *Physical Review B*, vol. 54, no. 1, pp. 5–7, 1996.

[13] A. K. Singh, H. P. Liermann, Y. Akahama, and H. Kawamura, "Aluminum as a pressure-transmitting medium cum pressure standard for x-ray diffraction experiments to 200 GPa with diamond anvil cells," *Journal of Applied Physics*, vol. 101, no. 12, pp. 1–6, 2007.

[14] X. Huang, F. Li, Q. Zhou et al., "Thermal equation of state of molybdenum determined from in situ synchrotron X-ray diffraction with laser-heated diamond anvil cells," *Scientific Reports*, vol. 6, Article ID 19923, 2016.

[15] X. Zhang, Z. Liu, K. Jin et al., "Solid phase stability of molybdenum under compression: sound velocity measurements and first-principles calculations," *Journal of Applied Physics*, vol. 117, 2015.

[16] K. D. Litasov, P. N. Gavryushkin, P. I. Dorogokupets et al., "Thermal equation of state to 33.5 GPa and 1673 K and thermodynamic properties of tungsten," *Journal of Applied Physics*, vol. 113, no. 13, Article ID 133505, 2013.

[17] N.-Y. Ko, J.-M. Hwang, and Y.-H. Ko, "Behavior of copper under high pressure: experimental and theoretical analyses," *Current Applied Physics*, vol. 31, pp. 93–98, 2021.

[18] H. Cynn and C.-S. Yoo, "Equation of state of tantalum to 174 GPa," *Physical Review B*, vol. 59, no. 13, pp. 8526–8529, 1999.

[19] M. Matsui, "High temperature and high pressure equation of state of gold," *Journal of Physics: Conference Series*, vol. 215, 2010.

[20] Z.-L. Liu, Y.-P. Tao, X.-L. Zhang, and L.-C. Cai, "High-pressure phase diagram of gold from first-principles calculations: converging to an isotropic atomic stacking order," *Computational Materials Science*, vol. 114, pp. 72–78, 2016.

[21] D. Jiang, S. Zhong, W. Xiao, D. Liu, M. Wu, and S. Liu, "Structural, mechanical, electronic, and thermodynamic properties of pure tungsten metal under different pressures: a first-principles study," *International Journal of Quantum Chemistry*, vol. 120, no. 13, Article ID e26231, 2020.

[22] A. A. Maradudin, E. W. Montroll, and W. G.H., "Theory of lattice dynamics in the harmonic approximation," *Solid State Physics*, vol. Supp. 3, 1963.

[23] C. Kittel, *Introduction to Solid State Physics*, John Wiley & Sons., 8th edition, 2004.

[24] K. Devlal, "High pressure and high temperature equation of state for metals," *Journal of Engineering, Computers & Applied Sciences*, vol. 2, no. 8, pp. 8–16, 2013.

[25] G. Leibfried and W. Ludwig, "Theory of anharmonic effects in crystals," *Solid State Physics - Advances in Research and Applications*, vol. 12, no. C, pp. 275–444, 1961.

[26] S. Kazanc and S. Ozgen, "Pressure effect on phonon frequencies in some transition metals: A molecular dynamics study," *Physica B: Condensed Matter*, vol. 365, no. 1–4, pp. 185–192, 2005.

[27] S. K. Jalal, A. M. Al-Sheikh, and R. H. Al-Saqa, "High pressure effects on the phonon frequency spectrum of silicon nanoparticle," *Iranian Journal of Science and Technology, Transaction A: Science*, vol. 45, no. 1, pp. 391–396, 2021.

[28] S. J. AL-Faris, R. H. Al-Saqa, H. M. Mohmad, and S. Kareem, "High pressure effects on the structural properties of GaN compound using equations of state," *International Journal of Thermodynamics*, vol. 25, no. 1, pp. 79–84, 2022.

[29] S. K. Saxena, "Pressure–volume equation of state for solids," *Journal of Physics and Chemistry of Solids*, vol. 65, no. 8-9, pp. 1561–1563, 2004.

[30] F. D. Stacey and P. M. Davis, "High pressure equations of state with applications to the lower mantle and core," *Physics of the Earth and Planetary Interiors*, vol. 142, no. 3-4, pp. 137–184, 2004.

[31] K. Kholiya, J. Chandra, and S. Verma, "Analysis of equation of states for the suitability at high pressure: MgO as an example," *The Scientific World Journal*, vol. 2014, Article ID 289353, 5 pages, 2014.

[32] A. Kantor, I. Kantor, A. Kurnosov et al., "Anelasticity of Fe_xO at high pressure," *Applied Physics Letters*, vol. 93, no. 3, Article ID 034106, 2008.

[33] W. B. Holzapfel, M. Hartwig, and W. Sievers, "Equations of state for Cu, Ag, and Au for wide ranges in temperature and pressure up to 500 GPa and above," *Journal of Physical and Chemical Reference Data*, vol. 30, no. 2, pp. 515–529, 2001.

[34] K. Y. Kim and A. L. Ruoff, "Isothermal equations of state of potassium," *Journal of Applied Physics*, vol. 52, no. 1, pp. 245–249, 1981.

[35] K. Syassen and W. B. Holzapfel, "Isothermal compression of Al and Ag to 120 kbar," *Journal of Applied Physics*, vol. 49, no. 8, pp. 4427–4430, 1978.

[36] A. Dewaele, P. Loubeyre, and M. Mezouar, "Equations of state of six metals above 94 GPa," *Physical Review B*, vol. 70, no. 9, Article ID 094112, 2004.

[37] H. K. Mao, P. M. Bell, J. W. Shaner, and D. J. Steinberg, "Specific volume measurements of Cu, Mo, Pd, and Ag and calibration of the ruby R_1 fluorescence pressure gauge from 0.06 to 1 Mbar," *Journal of Applied Physics*, vol. 49, no. 6, pp. 3276–3283, 1978.

[38] A. Dewaele, M. Torrent, P. Loubeyre, and M. Mezouar, "Compression curves of transition metals in the Mbar range: experiments and projector augmented-wave calculations," *Physical Review B*, vol. 78, no. 10, Article ID 104102, 2008.

[39] F. Birch, "Finite elastic strain of cubic crystals," *Physical Review*, vol. 71, no. 11, pp. 809–824, 1947.

[40] F. Birch, "*Section of geology and mineralogy*: elasticity and constitution of the Earth's Interior*," *Transactions of the New York Academy of Sciences*, vol. 14, no. 2 Series II, pp. 72–76, 1951.

[41] L. Gerward, "The bulk modulus and its pressure derivative for 18 metals," *Journal of Physics and Chemistry of Solids*, vol. 46, no. 8, pp. 925–927, 1985.

[42] P. K. Singh and A. Dwivedi, "Pressure derivatives of bulk modulus for materials at extreme compression," *Indian Journal of Pure & Applied Physics*, vol. 50, pp. 734–738, 2012.

[43] J. Shanker and M. Kumar, "Thermodynamic approximations in high-pressure and high-temperature physics of solids," *Physica Status Solidi (B)*, vol. 179, no. 2, pp. 351–356, 1993.

[44] C. E. Monfort III and C. A. Swenson, "An experimental equation of state for potassium metal," *Journal of Physics and Chemistry of Solids*, vol. 26, no. 2, pp. 291–301, 1965.

[45] P. A. Smith and C. S. Smith, "Pressure derivatives of the elastic constants of potassium," *Journal of Physics and Chemistry of Solids*, vol. 26, no. 2, pp. 279–289, 1965.

[46] S. N. Vaidya, I. C. Getting, and G. C. Kennedy, "The compression of the alkali metals to 45 kbar," *Journal of Physics and Chemistry of Solids*, vol. 32, no. 11, pp. 2545–2556, 1971.

[47] J. Gal, "Utilizing the Lindemann–Gilvarry criterion for parameterization of the equations of state of noble gases Ar, Xe and Kr," *ArXiv*, 2019.

[48] L. C. Ming, D. Xiong, and M. H. Manghnani, "Isothermal compression of Au and Al to 20 GPa," *Physica B+C*, vol. 139-140, pp. 174–176, 1986.
[49] J. F. Thomas Jr., "Third-order elastic constants of aluminum," *Physical Review*, vol. 175, no. 3, pp. 955–962, 1968.
[50] J. D. Silversmith and B. L. Averbach, *Pressure Dependence of the Elastic Constants of Beryllium and Beryllium-Copper Alloys*, p. 567, 1970.
[51] O. Schulte and W. B. Holzapfel, "Effect of pressure on the atomic volume of Zn, Cd, and Hg up to 75 GPa," *Physical Review B*, vol. 53, no. 2, pp. 569–580, 1996.
[52] G. C. Kennedy and R. N. Keeler, *American Institute of Physics Handbook*, D. E. Gray, Ed., pp. 4–39, McGraw-Hill, New York, 3rd edition, 1972.
[53] Y. Hiki and A. V. Granato, "Anharmonicity in noble metals; higher order elastic constants," *Physical Review*, vol. 144, no. 2, pp. 411–419, 1966.
[54] L.-G. Liu, M. Liu, H. Verbeek, Ch. Höffner, and G. Will, "Comparative compressibility of Cu, Ag and Au," *Journal of Physics and Chemistry of Solids*, vol. 51, no. 5, pp. 435–438, 1990.
[55] O. Teppo and P. Taskinen, "Critical evaluation of the thermodynamic properties of cobalt–gold alloys," *Scandinavian Journal of Metallurgy*, vol. 16, no. 6, pp. 257–261, 1987.
[56] D. Antonangeli, L. R. Benedetti, D. L. Farber et al., "Anomalous pressure evolution of the axial ratio c/a in hcp cobalt: interplay between structure, magnetism, and lattice dynamics," *Applied Physics Letters*, vol. 92, no. 11, Article ID 111911, 2008.
[57] C. S. Yoo, H. Cynn, P. Söderlind, and V. Iota, "New β(fcc)-cobalt to 210 GPa," *Physical Review Letters*, vol. 84, no. 18, pp. 4132–4135, 2000.
[58] S. Ono, "First-principles molecular dynamics calculations of the equation of state for tantalum," *International Journal of Molecular Sciences*, vol. 10, no. 10, pp. 4342–4351, 2009.
[59] K. W. Katahara, M. H. Manghnani, and E. S. Fisher, "Pressure derivatives of the elastic moduli of niobium and tantalum," *Journal of Applied Physics*, vol. 47, no. 2, pp. 434–439, 1976.
[60] S. N. Vaboya and G. C. Kennedy, "Compressibility of 18 metals to 45 kbar *," *Journal of Physics and Chemistry of Solids*, vol. 31, no. 10, pp. 2329–2345, 1970.
[61] L.-C. Ming and M. H. Manghnani, "Isothermal compression of bcc transition metals to 100 kbar," *Journal of Applied Physics*, vol. 49, no. 1, pp. 208–212, 1978.
[62] K. D. Litasov, P. I. Dorogokupets, E. Ohtani et al., "Thermal equation of state and thermodynamic properties of molybdenum at high pressures," *Journal of Applied Physics*, vol. 113, no. 9, Article ID 093507, 2013.
[63] T. S. Sokolova, P. I. Dorogokupets, and K. D. Litasov, "Self-consistent pressure scales based on the equations of state for ruby, diamond, MgO, B2–NaCl, as well as Au, Pt, and other metals to 4 Mbar and 3000 K," *Russian Geology and Geophysics*, vol. 54, no. 2, pp. 181–199, 2013.
[64] Z.-Y. Zeng, C.-E. Hu, L.-C. Cai, X.-R. Chen, and F.-Q. Jing, "Lattice dynamics and thermodynamics of molybdenum from first-principles calculations," *Journal of Physical Chemistry B*, vol. 114, no. 1, pp. 298–310, 2010.
[65] L. Dubrovinsky, T. Boffa-Ballaran, K. Glazyrin et al., "Single-crystal X-ray diffraction at megabar pressures and temperatures of thousands of degrees," *High Pressure Research*, vol. 30, no. 4, pp. 620–633, 2010.
[66] S. S. Kushwah, M. P. Sharma, and Y. S. Tomar, "An equation of state for molybdenum and tungsten," *Physica B: Condensed Matter*, vol. 339, no. 4, pp. 193–197, 2003.
[67] I. Y. Alkammash, "Evaluation of pressure and bulk modulus for alkali halides under high pressure and temperature using different EOS," *Journal of the Association of Arab Universities for Basic and Applied Sciences*, vol. 14, no. 1, pp. 38–45, 2013.
[68] L. C. Ming and M. H. Manghnani, "Isothermal compression and phase transition in beryllium to 28.3 GPa," *Journal of Physics F: Metal Physics*, vol. 14, no. 1, 1984.
[69] D. L. Heinz and R. Jeanloz, "The equation of state of the gold calibration standard," *Journal of Applied Physics*, vol. 55, no. 4, pp. 885–893, 1984.
[70] K. Takemura and A. Dewaele, "Isothermal equation of state for gold with a He-pressure medium," *Physical Review B*, vol. 78, no. 10, Article ID 104119, 2008.
[71] P. W. Bridgman, "Linear compression to 30,000 kg/cm^2, including relatively incompressible substances," *Proceedings of the American Academy of Arts and Sciences*, vol. 77, no. 6, pp. 189–234, 1949.
[72] J. Xu, H. Mao, and P. M. Bell, "Position-sensitive X-ray diffraction: hydrostatic compressibility of argon, tantalum, and copper to 769 kbar," *High Temperatures-High Pressures*, vol. 16, p. 495, 1984.
[73] E. Y. Tonkov and E. G. Ponyatovsky, "Phase transformations of elements under high pressure," in *Phase Transformations of Elements Under High Pressure*, p. 390, CRC Press, Boca Raton, 1st edition, 2004.
[74] P. Söderlind and J. A. Moriarty, "First-principles theory of Ta up to 10 Mbar pressure: structural and mechanical properties," *Physical Review B*, vol. 57, no. 17, pp. 10340–10350, 1998.
[75] Y. K. Vohra and A. L. Ruoff, "Phase transitions and equations of state at multimegabar pressures," *High Pressure Research*, vol. 4, no. 1–6, pp. 296–299, 1990.
[76] X. Qi, N. Cai, T. Chen, S. Wang, and B. Li, "Experimental and theoretical studies on the elasticity of tungsten to 13 GPa," *Journal of Applied Physics*, vol. 124, no. 7, Article ID 075902, 2018.
[77] A. J. C. Wilson, "A handbook of lattice spacings and structures of metals and alloys by W. B. Pearson," *Acta Crystallographica*, vol. 12, no. 2, Article ID 174, 1959.
[78] K. R. Sharma, "On thermodynamic analysis of substances with negative coefficient of thermal expansion," *Engineering*, vol. 05, no. 11, pp. 844–849, 2013.
[79] O. D. Neĭkov, Ed., *Handbook of Non-Ferrous Metal Powders: Technologies and Applications*, Elsevier, 2nd edition, 2019.